RAFFLES BULLETIN OF ZOOLOGY **65**: 440–454
Date of publication: 4 September 2017
http://zoobank.org/urn:lsid:zoobank.org:pub:069160EB-BA10-414D-87B4-0CC7DE25E53C

An integrative description of a limnoterrestrial tardigrade from the Philippines, *Mesobiotus insanis*, new species (Eutardigrada: Macrobiotidae: *harmsworthi* group)

Marc A. Mapalo[1,3*], Daniel Stec[2], Denise Mirano-Bascos[1] & Łukasz Michalczyk[2]

Abstract. The Philippines is considered a country with high biodiversity and endemism. However, the status of its tardigrade fauna is still practically unknown. In this study, a limnoterrestrial eutardigrade, *Mesobiotus insanis*, new species, from Diliman, Quezon City, located on the largest island in the Philippine Archipelago is described. Integrative taxonomy, via the combined morphological and morphometric analyses (imaging via phase contrast [PCM] and scanning electron microscopy [SEM]) aided with a molecular analysis (DNA barcoding of the *18S rRNA, 28S rRNA, ITS-2*, and *COI* markers), was employed to verify the status of the population as a new species. *Mesobiotus insanis*, new species, differs from its congeners mainly by its unique egg morphology characterised by an exceptionally complex sculpturing of the eggshell areolae in addition to other morphometric characters. The molecular analysis showed that the new species is genetically closest to *Mesobiotus philippinicus* Mapalo, Stec, Mirano-Bascos & Michalczyk, 2016, recently described also from the Philippines.

Key words. Asia, integrative taxonomy, *Mesobiotus insanis*, *Mesobiotus philippinicus*, Tardigrada

INTRODUCTION

The Philippines is considered as one of the megadiverse countries in terms of species numbers and endemism levels (Mittermeier et al., 1997; Posa et al., 2008). The diversity of invertebrate species alone in the country is estimated to be at ca. 35,000 (Brown & Diesmos, 2009). However, information on the Philippine tardigrade fauna is almost non-existent. So far, only one limnoterrestrial eutardigrade, *Mesobiotus philippinicus* Mapalo, Stec, Mirano-Bascos & Michalczyk, 2016, has been characterised in detail and reported from the Philippines (Mapalo et al., 2016). Considering the degree of biodiversity in the country, it is only reasonable to expect that many more tardigrade species inhabit the Philippines that are yet to be discovered.

In 2016, a new genus, *Mesobiotus*, was erected from within the cosmopolitan and polyphyletic genus *Macrobiotus* (Vecchi et al., 2016). The current 56 species of the genus (Degma et al., 2016) are characterised by Y-type double claws with a common tract and an internal septum in the claw base, cuticle without pores, 10 peribuccal lamellae, three roundish macroplacoids with a large microplacoid situated close to the third macroplacoid, and freely-laid eggs with conical or hemispherical processes. This genus consists of two species complexes, the *harmsworthi* and *furciger* groups, both previously recognised as groups within *Macrobiotus*. The main goal of this paper is to describe a new limnoterrestrial eutardigrade species from the Philippines using an integrative approach. The description involves morphological and morphometric analyses via phase contrast (PCM) and scanning electron microscopy (SEM) as well as DNA barcoding. The new species belongs to the *harmsworthi* group and can be distinguished from its congeners by the exceptionally complex sculpturing of the egg shell areolae that are in the form of rose-shaped whorls.

MATERIAL AND METHODS

Sample and specimens. A moss sample was collected from a tree trunk in the University of the Philippines, Diliman, Quezon City, Philippines in May 2014. An isogenic culture was established following the methods described by Mapalo et al. (2016). Briefly, a single female with mature oocytes was isolated and placed in a Petri dish lined with a 2% agar made with a KCM solution, The dish was filled with a thin layer of distilled, deionised water (ddH_2O) and some of the original moss fragments and rotifers found in the sample. The culture was then regularly checked for eggs and new individuals. Three new females with mature oocytes from this culture were used to create three individual isogenic subcultures that from then on were fed with *Chlorella* sp. (Aquatic Biotechnology Laboratory, National Institute of Molecular Biology and Biotechnology, Philippines). Individuals and eggs were then randomly extracted from all

[1]National Institute of Molecular Biology and Biotechnology, College of Science, University of the Philippines, Diliman, Quezon City, Philippines 1101; Email: marcmapalo@mbb.upd.edu.ph (*corresponding author)

[2]Institute of Zoology and Biomedical Research, Jagiellonian University, Gronostajowa 9, 30-387 Kraków, Poland

[3]Current affiliation: MEME, University of Groningen, Groningen 9712 CP, Netherlands

ISSN 2345-7600 (electronic) | ISSN 0217-2445 (print)

three subcultures and randomly split into three groups, for different types of analyses: (i) imaging and morphometry with PCM, (ii) imaging with SEM, and (iii) DNA sequencing.

Microscopy and imaging. Specimens for PCM were mounted on microscope slides with a small drop of Hoyer's medium prepared according to Morek et al. (2016) and secured with a cover slip. Slides were then dried for five days at 60°C in an incubator. Dried slides were sealed with transparent nail polish and examined under a Nikon Eclipse 50i phase contrast light microscope associated with a Nikon Digital Sight DS-L2 digital camera.

Eggs for SEM analysis were processed according to the protocol by Stec et al. (2015). Briefly, specimens first went through a water/ethanol and an ethanol/acetone series, followed by CO_2 critical point drying, and finally they were sputter coated with a thin layer of gold. Specimens were examined under high vacuum in a Versa 3D DualBeam Scanning Electron Microscope at the ATOMIN facility of the Jagiellonian University, Kraków, Poland.

All figures were assembled in Corel Photo-Paint X6, ver. 16.4.1.1281. For deep structures that could not be fully focused in a single photograph, a series of 2–6 images were taken every ca. 0.2 µm and then assembled into a single deep-focus image.

Morphometrics and morphological nomenclature. All measurements are given in micrometres (µm). Structures were measured only if their orientation was suitable. Sample size was chosen following Stec et al. (2016a). Body length was measured from the anterior extremity to the end of the body, excluding the hind legs. The terminology used to describe oral cavity armature, and later used in differential diagnoses, follows Michalczyk & Kaczmarek (2003). Buccal tube length and the level of the stylet support insertion point were measured according to Pilato (1981). Buccal tube width was measured as the external and internal diameter at the level of the stylet support insertion point. Macroplacoid length sequence is given according to Kaczmarek et al. (2014). Lengths of claw branches were measured from the base of the claw (excluding the lunules) to the top of the primary branch including accessory points (Kaczmarek & Michalczyk, in press). The *pt* ratio is the ratio of the length of a given structure to the length of the buccal tube, expressed as a percentage (Pilato, 1981); these measurements are always given in italics in this paper. Distance between egg processes was measured as the shortest distance connecting the base edges of the two closest processes (Kaczmarek & Michalczyk, in press). Morphometric data were handled using the "Parachela" ver. 1.2 template available from the Tardigrada Register, www.tardigrada.net/register (Michalczyk & Kaczmarek, 2013).

Genotyping. Four standard gene markers were used for the integrative identification of the species – three nuclear markers: the small ribosome subunit (*18S rRNA*), the large ribosome subunit (*28S rRNA*), the internal transcribed spacer 2 (*ITS-2*), and one mitochondrial gene: cytochrome oxidase subunit I (*COI*). Genomic DNA was extracted from individual tardigrades using the NucleoSpin genomic DNA extraction Kit (Macherey-Nagel) following the manufacturer's protocol. For every PCR reaction, the solution contained 6.75 µL ddH_2O, 2 µL 10X Titanium Taq Buffer, 0.2 µL 10 mM dNTPs, 0.5 µL 10 µM forward primer, 0.5 µL 10 µM reverse primer, and 0.05 µL 50X Titanium Taq polymerase, and 1 µL of genomic DNA extract. For every PCR run, 1 µL ddH_2O was added instead of the template for the negative control. The primers are given in Table 1. Amplification was done using the PCR profiles shown in Table 2. Successfully amplified fragments were sent to First Base Co., Singapore for PCR clean-up and sequencing. All sequences were viewed using BioEdit 7.2.5 (Hall, 1999) to determine the region of the sequences with good quality chromatogram signals. Flanking sequences with overlapping peaks or unresolved bases were eliminated until all the remaining sequences were of acceptable quality.

Phenotypic comparative analysis. First, the dichotomous key for the *harmsworthi* group by Kaczmarek et al. (2011) was used to determine whether the isolated species had already been described. After the species could not be identified with the key, we compared it with original descriptions of the most similar *harmsworthi* group species: *Mesobiotus barbarae* (Kaczmarek, Michalczyk, & Degma, 2007), *M. hieronimi* (Pilato & Claxton, 1988), *M. hilariae* Vecchi, Cesari, Bertolani, Jönsson, Rebecchi, & Guidetti, 2016, *M. nuragicus* (Pilato & Sperlinga, 1975), *M. harmsworthi obscurus* (Dastych, 1985), *M. ovostriatus* (Pilato & Patanè, 1997), *M. pseudoliviae* (Pilato & Binda, 1996), and *M. pseudonuragicus* (Pilato, Binda, & Lisi, 2004). Tardigrade taxonomy follows Bertolani et al. (2014).

Genotypic comparative analysis. First, the nuclear and mitochondrial gene sequences were subjected to a BLASTn and a BLASTx query, respectively (Altschul et al., 1990). Then, all published homologous sequences for species of the *harmsworthi* group were retrieved from GenBank (www.ncbi.nlm.nih.gov/genbank, Table 3) and used to calculate p-distances. For the *28S rRNA* comparison, only one sequence of *M. philippinicus* (KX129794 by Mapalo et al., 2016) was used since other published *28S rRNA* fragments correspond to a different region of the gene. For the *ITS-2* comparison, only the sequence of *M. philippinicus* (KX129795 by Mapalo et al., 2016) was used as no other ITS-2 sequences for the group are currently available. Additionally, the *COI* sequence was translated to polypeptides using EMBOSS Transeq (Rice et al., 2000; Goujon et al., 2010) to check against pseudogenes and to compare the amino acid sequences between the species. Mega6 (Tamura et al., 2013) was used to align all sequences using ClustalW Multiple Alignment tool (Thompson et al., 1994), and to calculate uncorrected p-distances.

Data deposition. Raw data underlying the description of *Mesobiotus insanis*, new species, are deposited in the Tardigrada Register (Michalczyk &Kaczmarek, 2013) under www.tardigrada.net/register/0043.htm. DNA sequences are deposited in GenBank.

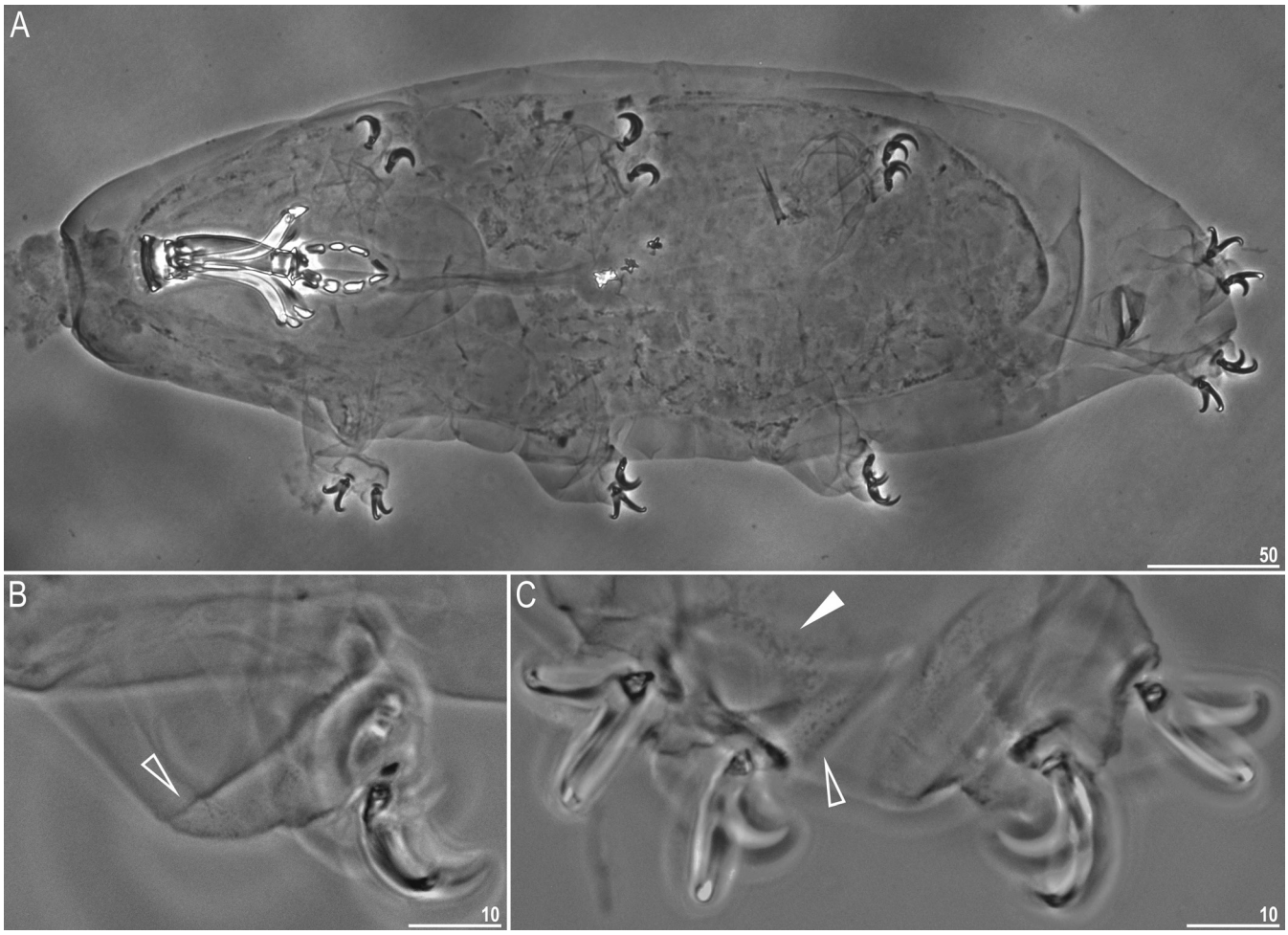

Fig. 1. *Mesobiotus insanis*, new species, PCM images of habitus and cuticle. A, dorso-ventral projection (holotype, PCM); B, dorsal cuticle above leg II; C, ventral cuticle of legs IV. Empty arrowheads indicate granulation; the filled arrowhead indicates the horse-shoe shaped structure connecting the anterior and the posterior claw. Scale bars in μm.

TAXONOMY

Phylum Tardigrada Doyère, 1840

Class Eutardigrada Richters, 1926

Order Parachela Schuster, Nelson, Grigarick & Christenberry, 1980

Superfamily Macrobiotoidea Thulin, 1928 (in Marley et al., 2011)

Family Macrobiotidae Thulin, 1928

Genus *Mesobiotus* Vecchi, Cesari, Bertolani, Jönsson, Rebecchi & Guidetti, 2016

***Mesobiotus insanis* new species**
(Figs. 1–8)

Material examined. Holotype (slide number: PH.003.12), 29 paratypes (slide numbers: PH.003.03–04, 06, 08–13, 15–16, 20), and 29 eggs (slide numbers: PH.003.07, 22, PH.004.01–03; 6 eggs on SEM stubs) as well as 7 females processed for DNA sequencing. All examined individuals and eggs were derived from a single female isolated from moss on the trunk of a tree growing in the UP Science Park, near the College of Science Library, University of the Philippines, Diliman, Quezon City, Philippines (14°38′56.2″N, 121°04′10.3″E, 60 m asl). Coll. Marc Mapalo, Mika Berza and Cali Fernandez, May 2014.

Description of the new species. Animals (morphometrics in Table 4): Body white/transparent (Fig. 1A). Eyes absent in live individuals. Cuticle without pores. Granulation present on legs I–IV (Fig. 1B, C, empty arrowheads).

Buccal apparatus of *Macrobiotus*-type with ventral lamina and ten peribuccal lamellae (Fig. 2A). Oral cavity armature of the *harmsworthi* type, composed of three bands of teeth visible under PCM (Fig. 2). The first band of teeth appears as small granules arranged in several irregular rows along the anterior portion of the oral cavity and sometimes on the bases of the lamellae (Fig. 2B–E, filled arrowheads). Teeth in the second band appear as small ridges that are parallel to the main axis of the buccal tube and situated at the posterior portion of the oral cavity (Fig. 2B–E, empty arrowheads). Situated right after the second band of teeth and before the buccal tube opening is the third band of teeth (Fig. 2B–E, indented arrowheads), consisting of 3 dorsal thin

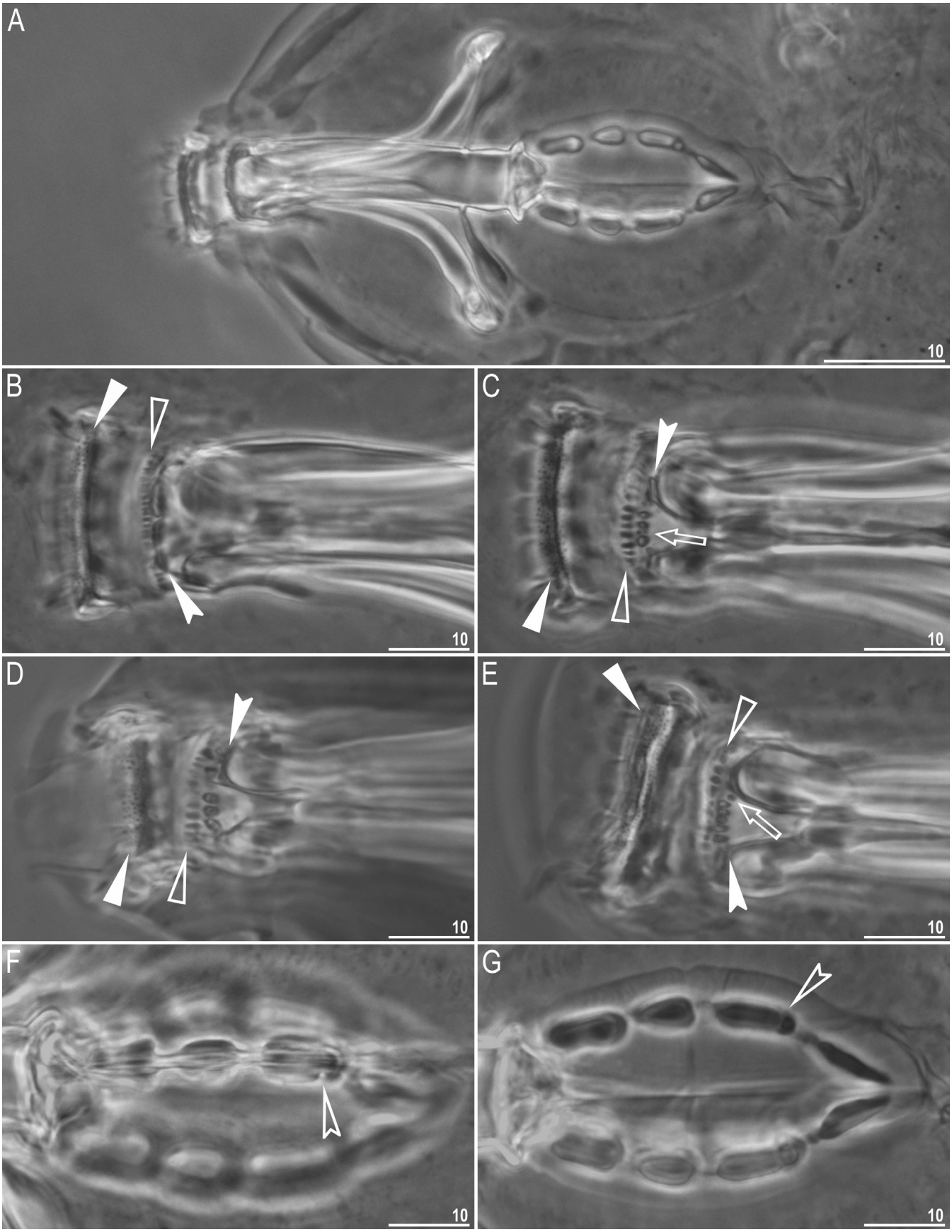

Fig. 2. *Mesobiotus insanis*, new species, PCM images of the buccal apparatus. A, an entire buccal apparatus (paratype); B, dorsal teeth; C–E, ventral teeth (in Fig C, D, E, the medio-ventral tooth is divided into three, four, and five oval teeth, respectively); F, ventral placoids; G, dorsal placoids. Filled flat arrowheads indicate the first band of teeth, empty flat arrowheads indicate the second band of teeth, filled indented arrowheads indicate the third band of teeth, empty arrows indicate the additional teeth in the third band, empty indented arrowheads indicate subterminal constrictions in the third macroplacoid. Scale bars in μm.

Table 1. Primers used for sequencing of *18S rRNA*, *28S rRNA*, *ITS-2*, and *COI* genes of *Mesobiotus insanis*, new species.

DNA Fragment	Primer Name	Primer Direction	Primer Sequence (5'-3')	Source
18S rRNA	SSU F7	forward	AAAGATTAAGCCATGCAT	Blaxter et al. (1998)
	SSU R9	reverse	AGCTGGAATTACCGCGGCTG	Blaxter et al. (1998)
28S rRNA	28SF0001	forward	ACCCVCYNAATTTAAGCATAT	Mironov et al. (2012)
	28SR0990	reverse	CCTTGGTCCGTGTTTCAAGAC	Mironov et al. (2012)
ITS-2	ITS3	forward	GCATCGATGAAGAACGCAGC	White et al. (1990)
	ITS4	reverse	TCCTCCGCTTATTGATATGC	White et al. (1990)
COI	LCO1490	forward	GGTCAACAAATCATAAAGATATTGG	Folmer et al. (1994)
	HCOoutout	reverse	GTAAATATATGRTGDGCTC	Prendini et al. (2005)

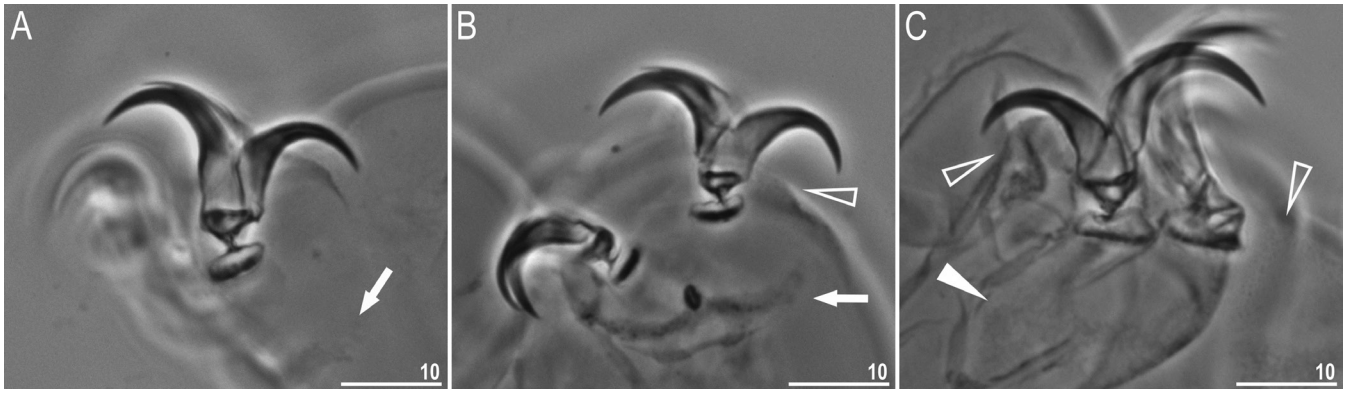

Fig. 3. *Mesobiotus insanis*, new species, PCM images of claws. A, claws I with smooth lunules; B, claws II with smooth lunules; C, claws IV with slightly crenulated lunules. Arrows indicate the W-shaped cuticular bars, the filled arrowhead indicates the horseshoe-shaped structure connecting the anterior and the posterior claw, the empty arrowheads indicate leg granulation. Scale in μm.

ridge teeth and 5–7 ventral teeth: 2 drop-shaped lateral teeth and 3–5 oval median teeth sometimes with additional teeth (Fig. 2B–E, arrow). Buccal tube rigid, with a ventral lamina and a thickening posterior to the stylet support insertion points. Pharyngeal apophyses, three macroplacoids and a microplacoid present in the muscle pharynx. All placoids equidistant from each other. In the ventral view, the first and the third macroplacoid are rod-shaped whereas the second macroplacoid is drop-like. The first macroplacoid is thinner anteriorly whereas the third macroplacoid has a sub-terminal constriction, which is visible in both the ventral and the dorsal view (Fig. 2F, G, empty indented arrowheads). The macroplacoid sequence is 2<1<3. The drop-like microplacoid is typically longer than the second macroplacoid (93% of the analysed animals, in the remaining 7% the second macroplacoid is equal to or slightly longer than the microplacoid).

Claws of the *Mesobiotus* type, with a peduncle connecting the claw to the lunula, a basal septum and well-developed accessory points on the primary branches (Fig. 3A–C). Lunules smooth under claws I–III (Fig. 3A, B) and slightly crenulated under claws IV (Fig. 3C). Single transverse W-shaped bars below claws I–III present (Fig. 3B, arrow), whereas a horseshoe-shaped structure connects the anterior and posterior lunules on claws IV (Figs. 1C, 3C, filled arrowheads).

Eggs (morphometrics in Table 5): Spherical, white, laid freely, with hemispherical to conical processes. The processes are equidistant from each other and vary in shape from low domes to high cones (Fig. 6A–L). The process surface is wrinkled and the wrinkles form a whorl that is clearly visible with SEM (Fig. 8A–F) but only appears as serrations on intersected process walls under PCM (Fig. 6A–H). Some eggs have smooth process surfaces under PCM (Fig. 6I–L). The labyrinthine layer within the process walls appears as reticulation under PCM, with meshes that vary in diameter considerably between eggs (Fig. 7A–D). A few scattered pores, especially in the basal portion of the process, are present in the external process wall (only clearly visible in SEM since in PCM the pores blend with the labyrinthine layer). Processes are terminated by at least 15 short, thin, and flexible filaments that are visible in both PCM (Fig. 6A–L) and SEM (Fig. 8A–F). The filaments are covered with tiny granules that are visible only in SEM (Fig. 8D, E). Processes are connected by 10–14 wide stripes (Figs. 7, 8A) with smooth surfaces in SEM (Fig. 8) but in PCM the stripes appear covered with mesh (Fig. 7) and sometimes large bubbles (Fig. 7D, empty arrowhead), which are all the representations of the labyrinthine layer below the surface of the stripes. The spaces between the connective stripes form single, complexly sculptured areolae on the egg surface (10–14 areolae around each process; Figs. 7, 8A–D, F). Each areola consists of a central rose-shaped whorl of fine

Table 2. PCR programmes used for the amplification of *18S rRNA*, *28S rRNA*, *ITS-2*, and *COI* gene fragments of *Mesobiotus insanis*, new species.

Step	18S rRNA			28S rRNA			ITS-2			COI		
	Temp [ºC]	Time [min:sec]	Cycles	Temp [ºC]	Time [min:sec]	Cycles	Temp [ºC]	Time [min:sec]	Cycles	Temp [ºC]	Time [min:sec]	Cycles
Initial denaturation	95	10:00	1	95	10:00	1	95	10:00	1	95	10:00	1
Denaturation	95	00:30	35	95	00:30	35	95	00:30	35	95	00:30	35
Annealing	55	00:30	35	50	00:30	35	50	00:30	35	41.1	00:30	35
Elongation	72	01:00	35	72	01:00	35	72	01:00	35	72	01:00	35
Final elongation	72	10:00	1	72	10:00	1	72	10:00	1	72	10:00	1

wrinkles (Figs. 7A–C, 8C–F) and porous surface around the whorl (Fig. 8D, F). Both whorls and pores are always clearly visible in SEM (Fig. 8C–F), however under PCM pores are never identifiable (they are below the resolution of light microscope) whereas whorls are visible only in some eggs (Fig. 7A–C).

Remarks. Eggs of the new species exhibit considerable variation in chorion morphology (Figs. 4–8). Given that the eggs were obtained in culture, it should be considered whether similar variability could be observed in the wild. The great majority of eutardigrade species descriptions provide images of only most typical eggs morphotypes, which may result in a conviction that eutardigrade eggs are characterised by low intra-specific variability. However, recent studies show that at least in some eutardigrade species, egg chorion may exhibit considerable morphological and morphometric variation in natural populations (Stec et al., 2017; Zawierucha et al., 2016). Moreover, eggs of *R. subanomalus* obtained by Stec et al. (2016b) in a laboratory culture showed the same extent of variation as eggs of the same species extracted from a moss sample by Stec et al. (2017), which suggests that *M. insanis*, new species, also may lay variable eggs in nature. Nevertheless, even if laboratory conditions indeed increased egg shell variability, the narrower natural variation would fall within that observed in the in vitro culture. In other words, a greater variability presented in the description would allow an easier identification of the species in the future.

DNA Sequences. A single haplotype was found for each of the four sequenced markers in all seven analysed individuals representing the three subcultures. The sequences were deposited in GenBank with the following reference numbers: *18S rRNA*, 499 bp long, MF441488; *28S rRNA*, 769 bp long, MF441489; *ITS*-2, 352 bp long, MF441490; *COI*, 771 bp long, MF441491.

Etymology. The name of the new species refers to its insanely complex egg morphology, never observed before in any other tardigrade species.

DISCUSSION

Phenotypic Differential Diagnosis. The presence of three rod-shaped macroplacoids, a relatively large microplacoid placed close to the third macroplacoid, and hemispherical or conical processes without finger-like projections on egg process apices places the new species in the *Mesobiotus harmsworthi* group (Kaczmarek et al., 2011). The new species differs from all its congeners by having whorl-shaped egg areolae. However, the new species, by having areolated eggs, is similar to the following taxa, but differs specifically from:

Mesobiotus barbarae (Kaczmarek, Michalczyk, & Degma, 2007), reported only from the type locality in the Dominican Republic, by: a wider buccal tube external diameter (8.6–16.0 µm [*pt=18.9–27.0*] in the new species vs. 3.4–8.3 µm [*pt=12.1–16.1*] in *M. barbarae*), a longer ventral lamina (30.6–45.5 µm [*pt=60.8–77.2*] in the new species vs. 16.9–32.7 µm [*pt=58.2–63.2*] in *M. barbarae*), a longer

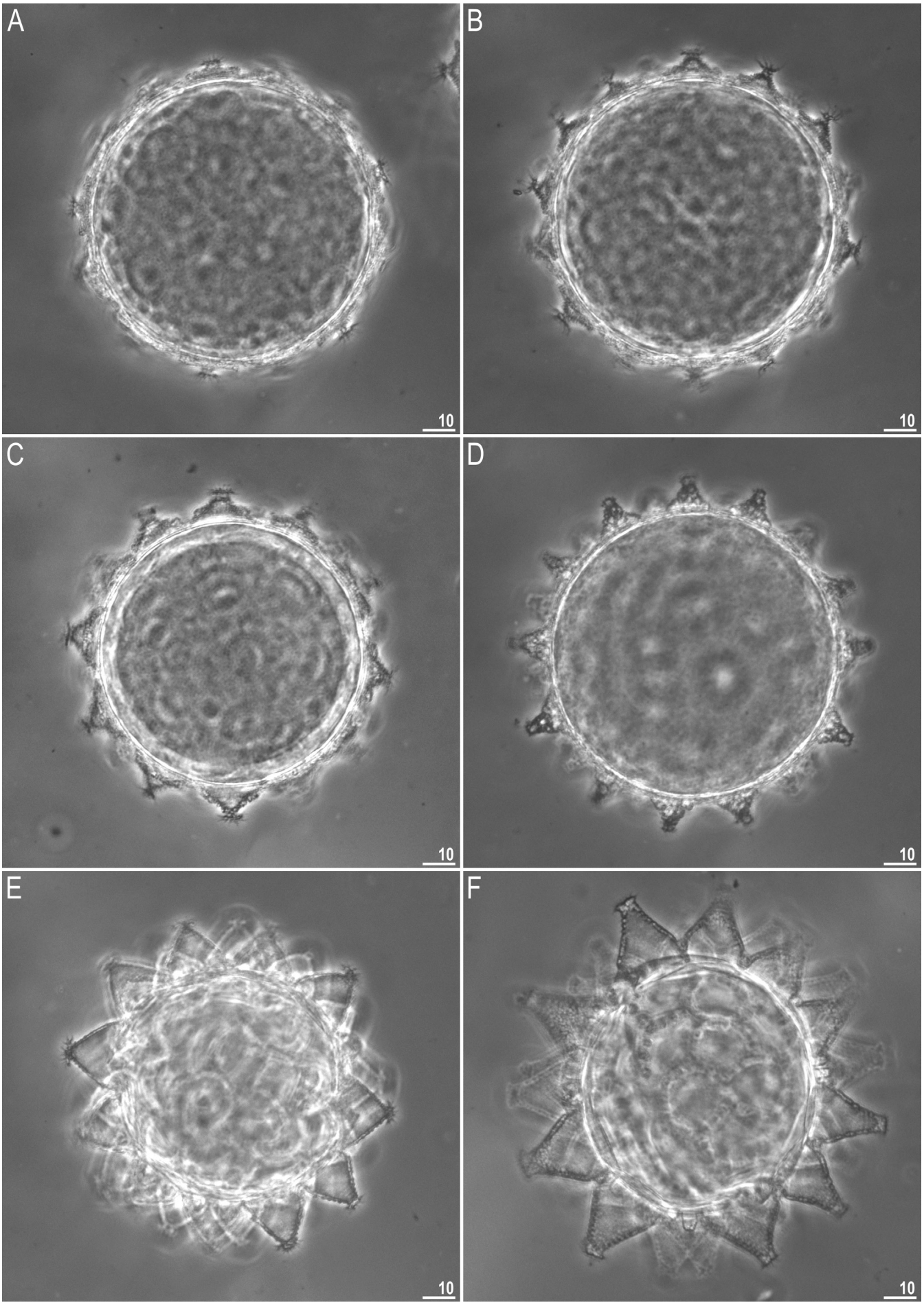

Fig. 4. *Mesobiotus insanis*, new species, PCM images of midsections of six different eggs. Scale bars in μm.

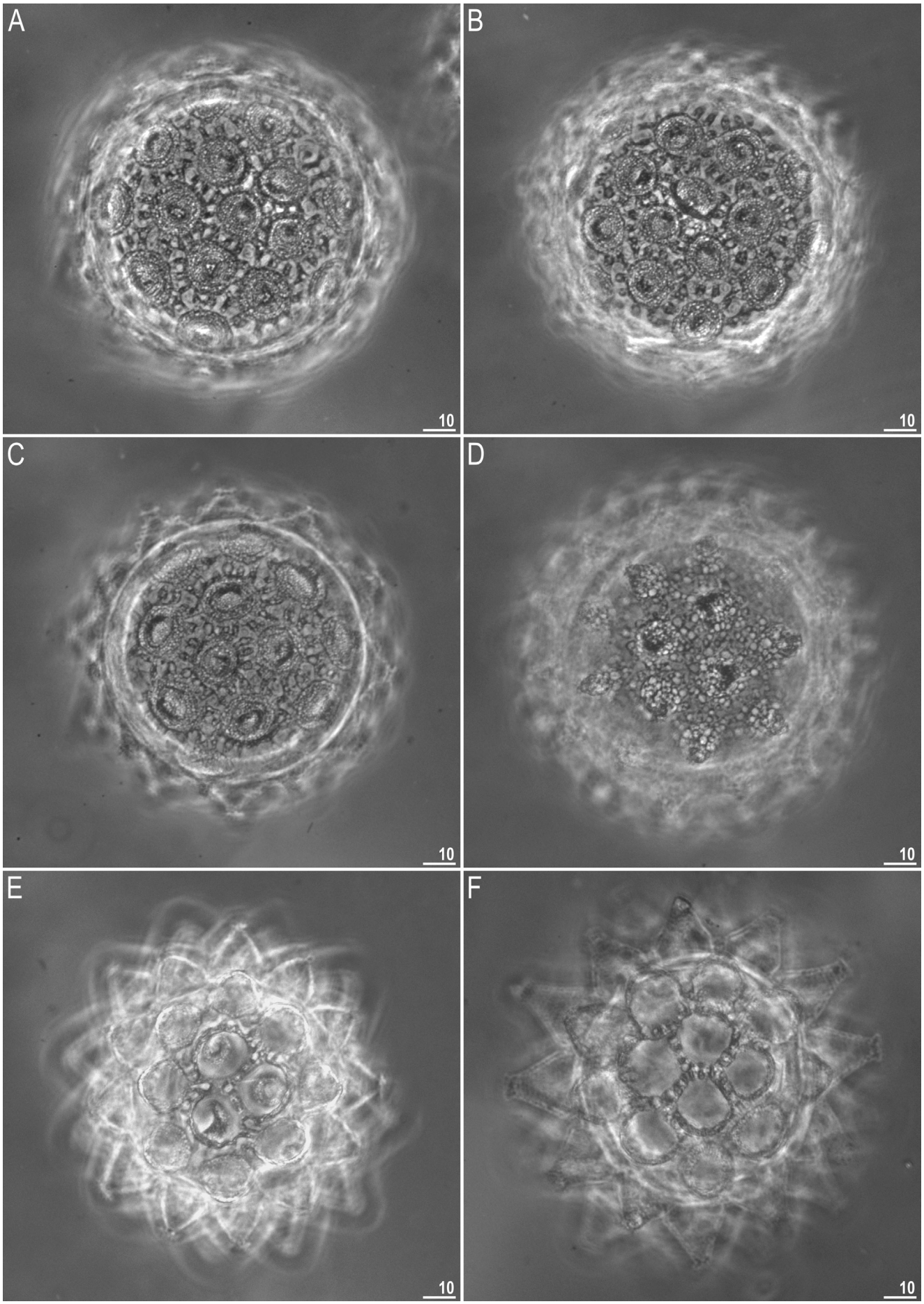

Fig. 5. *Mesobiotus insanis*, new species, PCM images of the surfaces of the eggs shown in Fig. 4 (respective letters indicate same eggs in both figures). Scale bars in μm.

Table 3. GenBank sequences of *18S rRNA*, *28S rRNA*, *ITS-2*, and *COI* gene fragments used for genetic comparison. [1]Bertolani et al. (2014), [2]Mapalo et al. (2016), [3]Vecchi et al. (2016)

	18S rRNA	28S rRNA	ITS-2	COI
Mesobiotus harmsworthi group	HQ604967–70[1]; KT226073–4[3]			
Mesobiotus cf. *mottai*	KT226072[3]			
Mesobiotus hilariae	KT226068–73[3]			KT226108[3]
Mesobiotus philippinicus	KX129793[2]	KX129794[2]	KX129795[2]	KX129796[2]
Mesobiotus polaris	KT226075–78[3]			

Table 4. Measurements (in µm) of selected morphological structures of individuals of *Mesobiotus insanis*, new species, mounted in Hoyer's medium (N—number of specimens/structures measured. Range refers to the smallest and the largest structure among all measured specimens; SD—standard deviation).

Character	N	Range		Mean		SD		Holotype	
		µm	pt	µm	pt	µm	pt	µm	pt
Body length	27	354–813	*745–1379*	542	*1004*	95	*136*	497	*976*
Buccopharyngeal tube									
Buccal tube length	30	44.2–60.7		53.7	–	5.0	–	51.0	–
Stylet support insertion point	30	37.0–50.4	*79.5–86.1*	44.2	*82.4*	4.2	*1.6*	42.8	*83.9*
Buccal tube external width	30	8.6–16.0	*18.9–27.0*	12.2	*22.6*	2.0	*2.0*	11.5	*22.6*
Buccal tube internal width	30	6.9–13.7	*15.6–23.1*	10.4	*19.2*	1.8	*1.9*	9.5	18.5
Ventral lamina length	24	30.6–45.5	*60.8–77.2*	37.5	*68.9*	4.4	*4.0*	33.6	*65.9*
Placoid lengths									
Macroplacoid 1	30	5.7–11.8	12.1–20.0	8.7	*16.2*	1.5	*2.0*	8.5	*16.7*
Macroplacoid 2	30	5.5–10.4	*9.3–17.6*	7.0	*12.8*	1.1	*1.6*	7.0	*13.7*
Macroplacoid 3	30	5.5–13.7	*6.6–23.2*	9.4	*17.1*	1.8	*2.9*	9.1	*17.8*
Microplacoid	30	4.9–10.9	*11.0–26.7*	8.5	*16.3*	1.5	*2.6*	8.3	*16.2*
Macroplacoid row	30	20.9–36.8	*47.1–62.5*	29.1	*54.0*	4.3	*4.0*	27.8	*54.6*
Placoid row	30	26.0–50.1	*58.7–85.0*	38.9	*72.2*	5.8	*5.4*	37.3	*73.2*
Claw 1 lengths									
External primary branch	20	12.1–19.5	*24.6–33.0*	15.5	*28.5*	2.1	*2.4*	14.2	*27.9*
External secondary branch	12	9.7–14.5	*19.7–26.0*	12.4	*23.3*	1.6	*1.8*	12.2	*23.9*
Internal primary branch	18	10.6–19.2	*21.1–32.7*	14.6	*27.4*	2.3	*3.1*	15.5	*30.4*
Internal secondary branch	13	9.1–17.5	18.5–29.5	12.3	*23.1*	2.3	*2.9*	12.5	*24.5*
Claw 2 lengths									
External primary branch	17	13.5–21.0	*27.8–37.2*	17.4	*32.2*	2.7	*3.0*	?	*?*
External secondary branch	10	10.8–16.3	*22.1–28.2*	13.4	*25.2*	2.2	*2.2*	12.9	*25.4*
Internal primary branch	14	10.0–18.6	*21.9–31.5*	14.2	*26.8*	2.3	*2.8*	?	*?*
Internal secondary branch	10	8.4–14.4	*18.4–24.2*	11.6	*22.2*	2.0	*2.1*	10.8	*21.1*
Claw 3 lengths									
External primary branch	14	13.2–24.0	*27.8–40.9*	17.2	*32.9*	3.2	*4.3*	17.0	33.4
External secondary branch	9	11.4–16.2	*23.2–27.3*	13.2	*25.2*	2.1	*1.6*	?	*?*
Internal primary branch	12	10.1–21.2	*20.2–35.9*	14.7	*27.7*	3.0	*4.0*	12.7	*24.9*
Internal secondary branch	8	9.3–15.5	*18.7–28.8*	12.2	*23.2*	2.5	*3.4*	9.5	*18.7*
Claw 4 lengths									
Anterior primary branch	21	11.6–25.1	*24.7–42.5*	18.8	*34.5*	3.0	*4.5*	17.2	*33.7*
Anterior secondary branch	16	11.1–16.7	*22.5–31.3*	14.4	*26.8*	1.8	*2.2*	13.9	*27.3*
Posterior primary branch	22	10.8–28.6	*22.8–48.5*	19.8	*36.5*	3.7	*4.9*	17.9	*35.1*
Posterior secondary branch	11	10.5–19.3	*23.8–32.8*	14.9	*27.0*	2.1	*2.7*	?	*?*

Table 5. Measurements (in μm) of selected morphological structures of eggs of *Mesobiotus insanis*, new species. mounted in Hoyer's medium (N—number of eggs/structures measured, Range refers to the smallest and the largest structure among all measured specimens; SD—standard deviation).

Character	N	Range	Mean	SD
Egg bare diameter	23	83.9–94.4	88.9	3.1
Egg full diameter	23	101.7–122.5	112.0	5.0
Process height	69	7.9–18.1	12.5	2.2
Process base width	69	14.6–24.0	19.3	2.4
Process base/height ratio	69	108%–255%	159%	31%
Distance between processes	69	1.0–8.3	3.9	1.7
Number of processes on the egg circumference	20	11–16	13.0	1.5

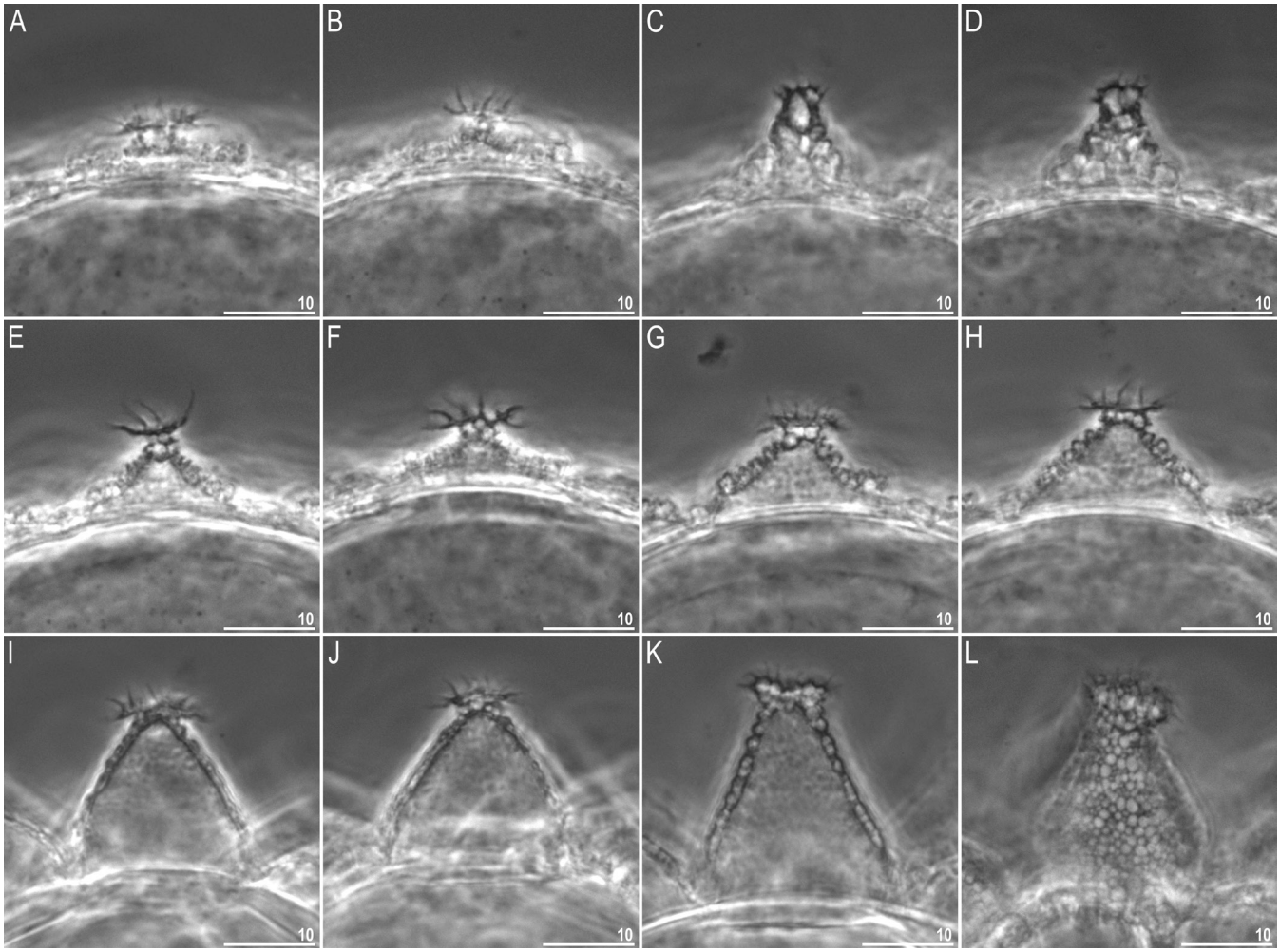

Fig. 6. *Mesobiotus insanis*, new species, PCM images of the midsection of processes from various eggs. Scale bars in μm.

microplacoid (4.9–10.0 μm [*pt=11.0–26.7*] in the new species vs. 2.0–5.1 μm [*pt=7.1–12.2*] in *M. barbarae*), a larger egg bare diameter (83.9–94.4 μm in the new species vs. 63.8–71.0 in *M. barbarae*), but shorter processes (7.9–18.1 μm in the new species vs. 18.4–26.5 μm in *M. barbarae*), a higher number of processes on the egg circumference (11–16 in the new species vs. 10 in *M. barbarae*), a higher number of areolae per egg process (10–14 in the new species vs. 5–6 in *M. barbarae*), and by a different morphology of egg process apices (divided into at least 15 filaments in the new species vs. single or bifurcated in *M. barbarae*).

Mesobiotus harmsworthi obscurus (Dastych, 1985), recorded only from the type locality in Svalbard, Norway, by: the absence of eyes, a wider buccal tube external diameter (8.6–16.0 μm in the new species vs. 7.0 μm in *M. harmsworthi obscurus*), the absence of supplementary small granular teeth between the second and the third band of teeth in the oral cavity, a different macroplacoid length sequence (2<1<3 in the new species vs. 2<1=3 in *M. harmsworthi obscurus*), a larger bare egg diameter (83.9–94.4 μm in the new species vs. 70–82 μm in *M. harmsworthi obscurus*), and by a higher number of areolae per egg process (10–14 in the new species vs. 6 in *M. harmsworthi obscurus*).

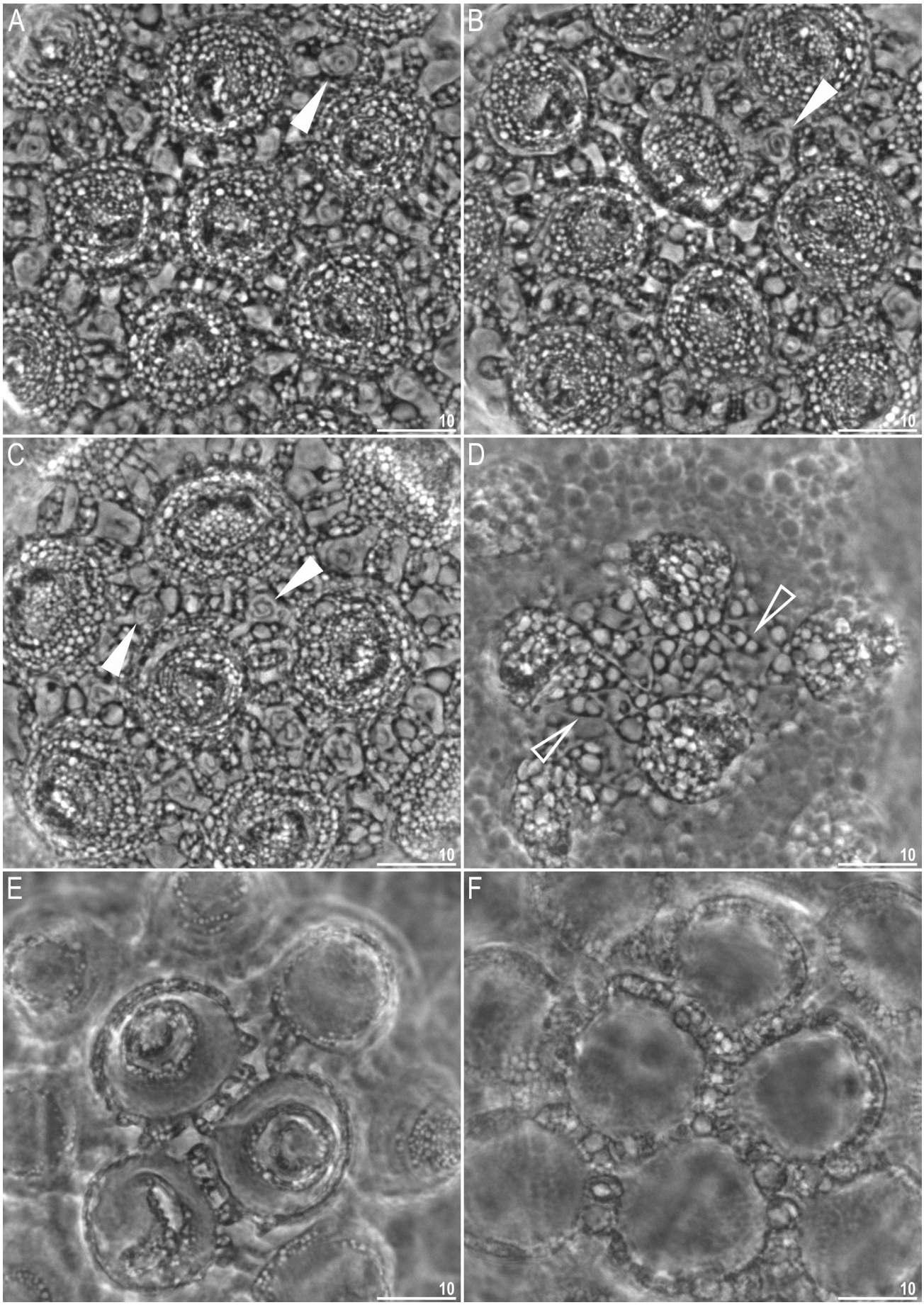

Fig. 7. *Mesobiotus insanis*, new species, magnified PCM images of the surface of the eggs shown in Fig. 4 (respective letters indicate same eggs in both figures). Filled arrowheads indicate the whorled sculpturing inside areolae; empty arrowheads indicate the bubble-like structures within the rims delimiting the areolae. Scale bars in μm.

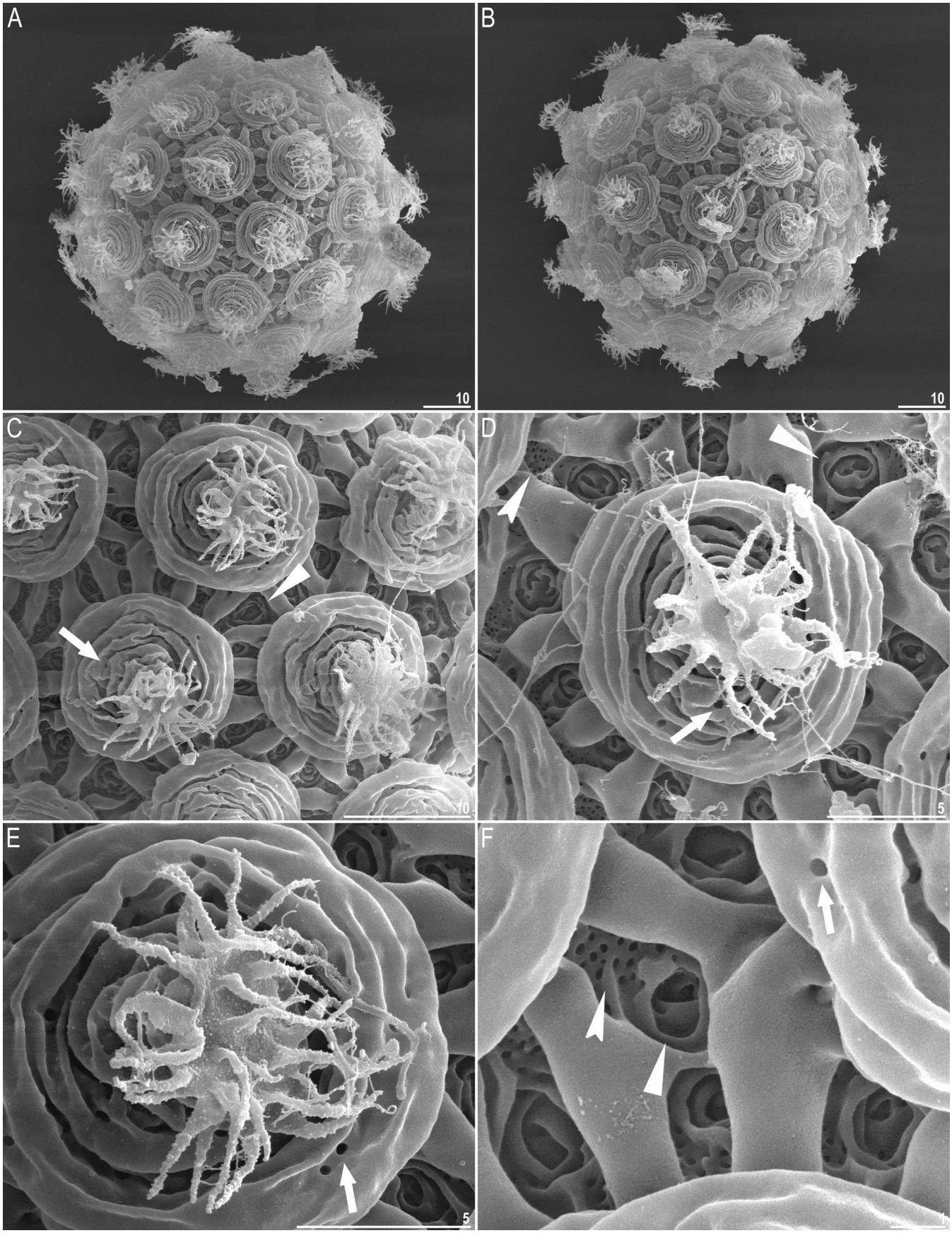

Fig. 8. *Mesobiotus insanis*, new species, SEM images of eggs. A, B, entire view of two different eggs; C, D, egg surface with processes; E, egg process; F, egg surface between processes, with evident pores and whorl-shaped sculpturing. Arrows indicate pores in the processes, flat arrowheads indicate the whorl-shaped surface inside the areolae, indented arrowheads indicate pores inside the areolae. Scale bars in μm.

Mesobiotus hieronimi (Pilato & Claxton, 1988), reported from the type locality in Australia and from South Georgia Island (Pilato & Claxton, 1988), by: the absence of eyes, more posterior stylet supports (*pt=79.5–86.1* in the new species vs. *pt=73.3–74.8* in *M. hieronimi*), a different macroplacoid length sequence (2<1<3 in the new species vs. 1≈2≈3 in *M. hieronimi*), a different lunulae IV morphology (crenulated in the new species vs. smooth in *M. hieronimi*), a larger bare egg diameter (83.9–94.4 µm in the new species vs. ca. 56.8 µm in *M. hieronimi*), but shorter processes (7.9–18.1 µm in the new species vs. 25.0–34.0 µm in *M. hieronimi*), a slightly higher number of processes on the egg circumference (11–16 in the new species vs. 9–12 in *M. hieronimi*), a higher number of areolae per egg process (10–14 in the new species vs. 6 in *M. hieronimi*), and by a different morphology of egg process apices (divided into at least 15 filaments in the new species vs. bifurcated in *M. hieronimi*).

Mesobiotus hilariae (Vecchi, Cesari, Bertolani, Jönsson, Rebecchi, & Guidetti, 2016), recorded only from the type locality in Antarctica, by: the absence of eyes, a different morphology of the ventral teeth in the third band (two lateral teeth and 3–5 median teeth in the new species vs. only 2 median teeth in *M. hilariae*), a wider buccal tube external diameter (8.6–16.0 µm [*pt=18.9–27*] in the new species vs. 2.0–3.0 µm [*7.1–8.6*] in *M. hilariae*), a different macroplacoid length sequence (2<1<3 in the new species vs. 2=3<1 in *M. hilariae*), the absence of swellings on legs, a different morphology of egg process apices (divided into at least 15 filaments in the new species vs. single or sometimes bifurcated in *M. hilariae*), and by a higher number of areolae per egg process (10–14 in the new species vs. 6 in *M. hilariae*).

Mesobiotus nuragicus (Pilato & Sperlinga, 1975), reported only from the type locality in Italy, by: the absence of eyes, a wider buccal tube external diameter (8.6–16.0 µm in specimens of 354–813 µm in length in the new species vs. 6.0 µm in *M. nuragicus* in specimen with 320 µm body length), a different macroplacoid length sequence (2<1<3 in the new species vs. 2<1=3 in *M. nuragicus*), a larger egg bare diameter (83.9–94.4 µm in the new species vs. 72.0 µm in *M. nuragicus*), and by a different morphology of egg process apices (divided into at least 15 filaments in the new species vs. divided into 2–5 tips in *M. nuragicus*).

Mesobiotus ovostriatus (Pilato & Patanè, 1997), recorded only from the type locality in Tierra del Fuego, by: the body colour (white in the new species *vs*. reddish in *M. ovostriatus*), the absence of eyes, a wider buccal tube external diameter (8.6–16.0 µm [*pt=18.9–27.0*] in the new species vs. 4.1–4.9 µm [*pt=11.85–13.82*] in *M. ovostriatus*), the presence of the first band of teeth in the oral cavity, a different macroplacoid length sequence (2<1<3 in the new species vs. 2<3<1 in *M. ovostriatus*), a longer microplacoid (4.9–10.9 µm [*pt=11.0–26.7*] in the new species vs. 2.3–2.9 µm [*pt=6.4–8.0*] in *M. ovostriatus*), a different lunulae IV morphology (crenulated in the new species vs. smooth in *M. ovostriatus*), a larger egg size (full diameter=101.7–122.5 *µm*, bare diameter=83.9–94.4 µm in the new species vs. 92.0–97.0 µm and 64.0–70.0 µm in *M. ovostriatus*), a different morphology of egg process apices (divided into at least 15 filaments in the new species vs. 1 long, narrow flexible terminal portion in *M. ovostriatus*), and by the absence of dots around the base of the processes.

Mesobiotus pseudoliviae (Pilato & Binda, 1996), reported only from the type locality in New Zealand, by: the absence of eyes, a different macroplacoid length sequence (2<1<3 in the new species vs. 2<3<1 in *M. pseudoliviae*), a larger bare egg diameter (83.9–94.4 µm in the new species vs. 72.0–78.0 µm in *M. pseudoliviae*), but shorter egg processes (7.9–18.1 µm in the new species vs. 42–56 µm in *M. pseudoliviae*), a higher number of processes on the egg circumference (11–16 in the new species vs. 8–9 in *M. pseudoliviae*), and by a different morphology of egg process apices (divided into at least 15 filaments in the new species vs. undivided in *M. pseudoliviae*).

Mesobiotus pseudonuragicus (Pilato, Binda, & Lisi, 2004), recorded only from the type locality in Seychelles, by: a wider buccal tube external diameter (8.6–16.0 µm [*pt=18.9–27.0*] in the new species vs. 6.6–6.8 µm [*pt=17.1–18.1*] in *M. pseudonuragicus*), a different macroplacoid length sequence (2<1<3 in the new species vs. 2<3<1 in *M. pseudonuragicus*), a different lunulae IV morphology (crenulated in the new species vs. smooth in *M. pseudonuragicus*), a larger egg size (full diameter=101.7–122.5 µm and bare diameter=83.9–94.4 µm in the new species vs. 82.8–104.8 µm and 53.8–72.6 µm in *M. pseudonuragicus*), a wider egg processes base (14.6–24.0 µm in the new species vs. 11.1–16 µm in *M. pseudonuragicus*), a higher number of areolae per egg process (10–14 in the new species vs. 5–7 in *M. pseudonuragicus*), and by the absence of dots around each egg processes.

Genotypic Differential Diagnosis. For all four sequenced markers, both BLAST and BLASTx analyses indicated *M. philippinicus* as the most closely related taxon to *M. insanis*. The *18S rRNA* p-distances between the new species and other *Mesobiotus* species ranged from 0.6% to 3.2% with the most similar being *M. philippinicus* and the least similar being *M.* cf. *mottai*, respectively. The *28S rRNA* and *ITS-2* p-distances between the new species *vs. M. philippinicus* were 6.8% and 24.6%, respectively. The *COI* p-distances between the new species and both *M. philippinicus* and *M. hilariae* ranged from 22.2% to 24.4% for the nucleotide sequences and were both equal to 11.6% for the amino acid sequences. Thus, overall, the observed p-distances strongly corroborate the phenotypic delineation of *M. insanis* from the compared species.

The close genetic relationship between *M. insanis*, new species, and *M. philippinicus* is not surprising, given the two species have been described from the same geographic area. However, the molecular distinctiveness of the two species is also supported not only by their molecular p-distances but also by their phenotypic divergence. Although *M. insanis*, new species, and *M. philippinicus* share a similar whorled wrinkling of the egg processes, they differ greatly in a number of morphological and morphometric traits. Among the most obvious is the absence of eyes in *M. insanis*, new

species, a 2<1<3 macroplacoid length sequence (2<3<1 in *M. philippinicus*), and the presence of egg areolae in the new species (wrinkled eggshell surface in *M. philippinicus*).

CONCLUSION

Combined morphological and molecular analyses support the erection of a new species of tardigrade from the Philippines. *Mesobiotus insanis*, new species, belongs to the *harmsworthi* group of the genus *Mesobiotus*. According to the molecular analysis, the new species is most closely related to *Mesobiotus philippinicus*, but sufficiently distinct to comprise a separate species. In addition, the two taxa exhibit clear phenotypic differences.

ACKNOWLEDGEMENTS

We would like to thank Diane Nelson and the second anonymous reviewer for their valuable comments and suggestions to the manuscript. We are grateful to Inés Daras for translating the original description of *M. nuragicus* from Italian. The study was supported by the National Institute of Molecular Biology and Biotechnology, University of the Philippines and by the Polish Ministry of Science and Higher Education via the *Iuventus Plus* programme (grant no. IP2014 017973).

LITERATURE CITED

Altschul SF, Gish W, Miller W, Myers EW & Lipman DJ (1990) Basic local alignment search tool. Journal of Molecular Biology, 215(3): 403–410.

Bertolani R, Guidetti R, Marchioro T, Altiero T, Rebecchi L, & Cesari M (2014) Phylogeny of Eutardigrada: New molecular data and their morphological support lead to the identification of new evolutionary lineages. Molecular Phylogenetics and Evolution, 76: 110–126. https://doi.org/10.1016/j.ympev.2014.03.006.

Blaxter M, De Ley P, Garey JR, Liu LX, Scheldeman P, Vierstraete A, Vanfleteren JR, Mackey LY, Dorris M, Frisse LM, Vida JT, & Thomas WK (1998) A molecular evolutionary framework for the phylum Nematoda. Nature, 392(6671): 71–75. https://dx.doi.org/10.1038/32160.

Brown RM & Diesmos AC (2009) Philippines, Biology. In: Gillespie RG & Clague DA (eds.) Encyclopedia of Islands. University of California Press, Berkeley, USA. Pp. 723–732.

Dastych H (1985) West Spitsbergen Tardigrada. Acta Zoologica Cracoviensia, 28: 169–214.

Degma P, Bertolani R & Guidetti R (2016) Actual checklist of Tardigrada species. http://www.tardigrada.modena.unimo.it/miscellanea/Actual%20checklist%20of%20Tardigrada.pdf. (Accessed 11 January 2017)

Doyère LMF (1840) Memoire sur les Tardigrades. I. Annales des Sciences Naturelles, Paris, Series 2, 14: 269–362.

Folmer O, Black M, Hoeh W, Lutz R & Vrijenhoek R (1994) DNA primers for amplification of mitochondrial cytochrome c oxidase subunit I from diverse metazoan invertebrates. Molecular Marine Biology and Biotechnology, 3: 294–299.

Goujon M, McWilliam H, Li W, Valentin F, Squizzato S, Paern J & Lopez R (2010) A new bioinformatics analysis tools framework at EMBL-EBI. Nucleic Acids Research 38, Supplement 2: W695–W699.

Hall TA (1999) Bioedit: A user-friendly biological sequence alignment editor and analysis program for Windows 95/98/NT. Nucleic Acids Symposium Series, 41: 95–98.

Kaczmarek Ł, Cytan J, Zawierucha K, Diduszko D & Michalczyk Ł (2014) Tardigrades from Peru (South America), with descriptions of three new species of Parachela. Zootaxa, 3790(2): 357–379. http://dx.doi.org/10.11646/zootaxa.3790.2.5.

Kaczmarek Ł & Michalczyk Ł (In press) The *Macrobiotus hufelandi* (Tardigrada) group revisited. Zootaxa.

Kaczmarek Ł, Michalczyk Ł & Degma P (2007) Description of a new tardigrade, *Macrobiotus barbarae* (Eutardigrada: Macrobiotidae) from the Dominican Republic. Annales Zoologici, 57(3): 363–369.

Kaczmarek Ł, Gołdyn B, Prokop ZM & Michalczyk Ł (2011) New records of Tardigrada from Bulgaria with the description of *Macrobiotus binieki* sp. nov. (Eutardigrada: Macrobiotidae) and a key to the species of the *harmsworthi* group. Zootaxa, 2781: 29–39.

Mapalo M, Stec D, Mirano-Bascos D, & Michalczyk Ł (2016) *Mesobiotus philippinicus* sp. nov, the first limnoterrestrial tardigrade from the Philippines. Zootaxa, 4126(3): 411–426. http://dx.doi.org/10.11646/zootaxa.4126.3.6

Marley NJ, McInnes SJ & Sands CJ (2011) Phylum Tardigrada: A re-evaluation of the Parachela. Zootaxa, 2819: 51–64.

Michalczyk Ł & Kaczmarek Ł (2003) A description of the new tardigrade *Macrobiotus reinhardti* (Eutardigrada, Macrobiotidae, *harmsworthi* group) with some remarks on the oral cavity armature within the genus *Macrobiotus* Schultze. Zootaxa, 331: 1–24. https://dx.doi.org/10.11646/zootaxa.331.1.1.

Michalczyk Ł & Kaczmarek Ł (2013) The Tardigrada Register: A comprehensive online data repository for tardigrade taxonomy. Journal of Limnology, 72(S1): 175–181. http://dx.doi.org/10.4081/jlimnol.2013.s1.e22.

Mironov SV, Dabert J & Dabert M. (2012) A new feather mite species of the genus *Proctophyllodes* Robin, 1877 (Astigmata: Proctophyllodidae) from the Long-tailed Tit *Aegithalos caudatus* (Passeriformes: Aegithalidae): morphological description with DNA barcode data. Zootaxa, 3253: 54–61.

Mittermeier RA, Robles-Gil P & Mittermeier CG (1997) Megadiversity: Earth's Biologically Wealthiest Nations. CEMEX, Mexico City, Mexico, 501 pp.

Morek W, Stec D, Gąsiorek P, Schill RO, Kaczmarek Ł & Michalczyk Ł (2016) An experimental test of eutardigrade preparation methods for light microscopy. Zoological Journal of the Linnean Society, 178(4): 785–793. http://dx.doi.org/10.1111/zoj.12457.

Pilato G (1981) Analisi di nuovi caratteri nello studio degli Eutardigradi. Animalia, 8: 51–57.

Pilato G & Binda MG (1996) Two new species and new records of *Macrobiotus* (Eutardigrada) from New Zealand. New Zealand Journal of Zoology, 23: 375–379.

Pilato G, Binda MG & Lisi O (2004) Notes on tardigrades of the Seychelles with the description of three new species. Italian Journal of Zoology, 71: 171–178.

Pilato G & Claxton SK (1988) Tardigrades from Australia. I. *Macrobiotus hieronimi* and *Minibiotus macularus*, two new species of eutardigrades. Animalia, 15(1): 83–89.

Pilato G & Patanè M (1997) *Macrobiotus ovostriatus*, a new species of eutardigrade from Tierra del Fuego. Bollettino delle sedute della Accademia gioenia di scienze naturali in Catania, 30(353): 263–268.

Pilato G & Sperlinga G (1975) Tardigradi muscicoli di Sardegna. Animalia, 2: 79–90.

Posa MRC, Diesmos AC, Sodhi NS & Brooks TM (2008) Hope for threatened tropical biodiversity: Lessons from the Philippines. Bioscience, 58(3): 231–240. http://dx.doi.org/10.1641/B580309.

Prendini L, Weygoldt P & Wheeler WC (2005) Systematics of the Damon *variegatus* group of African whip spiders (Chelicerata: Amblypygi): evidence from behaviour, morphology and DNA. Organisms, Diversity and Evolution, 5: 203–236.

Rice P, Longden I & Bleasby A (2000) EMBOSS: The European molecular biology open software suite. Trends in Genetics, 16(6): 276–277. https://dx.doi.org/10.1016/S0168-9525(00)02024-2.

Richters F (1926) Tardigrada. In: Kükenthal W & Krumbach T (eds.), Handbuch der Zoologie. Volume 3. Walter de Gruyter & Co., Berlin & Leipzig. Pp. 58–61.

Schuster RO, Nelson DR, Grigarick AA & Christenberry D (1980) Systematic criteria of the Eutardigrada. Transactions of the American Microscopical Society, 99: 284–303.

Stec D, Gąsiorek P, Morek W, Kosztyła P, Zawierucha K, Michno K, Kaczmarek Ł, Prokop ZM & Michalczyk Ł (2016a) Estimating optimal sample size for tardigrade morphometry. Zoological Journal of the Linnean Society, 178(4): 776–784. http://dx.doi.org/10.1111/zoj.12404.

Stec D, Morek W, Gąsiorek P, Kaczmarek Ł & Michalczyk Ł (2016b) Determinants and taxonomic consequences of extreme egg shell variability in *Ramazzottius subanomalus* (Biserov, 1985) (Tardigrada). Zootaxa, 4208(2): 176–188. https://dx.doi.org/10.11646/zootaxa.4208.2.5.

Stec D, Smolak R, Kaczmarek Ł & Michalczyk Ł (2015) An integrative description of *Macrobiotus paulinae* sp. nov. (Tardigrada: Eutardigrada: Macrobiotidae: *hufelandi* group) from Kenya. Zootaxa, 4052(5): 501–526. http://dx.doi.org/10.11646/zootaxa.4052.5.1

Stec D, Zawierucha K & Michalczyk Ł (2017) An integrative description of *Ramazzottius subanomalus* (Biserov, 1985) (Tardigrada) from Poland. Zootaxa, 4300(3): 403–420. https://dx.doi.org/10.11646/zootaxa.4300.3.4.

Tamura K, Stetcher G, Peterson D, Filipski A, & Kumar S (2013) MEGA6: Molecular Evolutionary Genetics Analysis Version 6.0. Molecular Biology and Evolution, 30(12): 2725–2729. https://dx.doi.org/10.1093/molbev/mst197.

Thompson JD, Higgins DG & Gibson TJ (1994) CLUSTAL W: Improving the sensitivity of progressive multiple sequence alignment through sequence weighting, position-specific gap penalties and weight matrix choice. Nucleic Acids Research, 22 (22): 4673–4680. http://dx.doi.org/10.1093/nar/22.22.4673.

Thulin G (1928). Über die Phylogenie und das System der Tardigraden. Hereditas, 11: 207–266.

Vecchi M, Cesari M, Bertolani R, Jönsoon KI & Guidetti R (2016) Integrative systematic studies on tardigrades from Antarctica identify new genera and new species within Macrobiotoidea and Echiniscoidea. Invertebrate Systematics, 30(4): 303–322.

White TJ, Bruns T, Lee S & Taylor J (1990) Amplification and Direct Sequencing of Fungal Ribosomal RNA Genes for Phylogenetics. In: Innis MA, Gelfand DH & Sninsky JJ (eds.) PCR Protocols: A Guide to Methods and Applications. Academic Press Inc., New York. Pp. 315–322.

Zawierucha K, Kolicka M & Kaczmarek Ł (2016) Re-description of the Arctic tardigrade *Tenuibiotus voronkovi* (Tumanov, 2007) (Eutardigrades; Macrobiotidae), with the first molecular data for the genus. Zootaxa, 4196(4): 498–510. http://dx.doi.org/10.11646/zootaxa.4196.4.2.